

---

# Position Paper

## Are Normalizing Flows the Key to Unlocking the Exponential Mechanism?

### A Path through the Accuracy-Privacy Ceiling Constraining Differentially Private ML

---

Robert A. Bridges <sup>\*1</sup> Vandy J. Tombs <sup>\*1</sup> Christopher B. Stanley <sup>1</sup>

#### Abstract

The state of the art and de facto standard for differentially private machine learning (ML) is differentially private stochastic gradient descent (DPSGD). Yet, the method is inherently wasteful. By adding noise to every gradient, it diminishes the overall privacy with every gradient step. Despite 15 years of fruitful research advancing the composition theorems, sub-sampling methods, and implementation techniques, adequate accuracy and privacy is often unattainable with current private ML methods. Meanwhile, the Exponential Mechanism (ExpM), designed for private optimization, has been historically sidelined from privately training modern ML algorithms primarily because ExpM requires sampling from a historically intractable density. Despite the recent discovery of Normalizing Flow models (NFs),

expressive deep networks for approximating intractable distributions, ExpM remains in the background. Our position is that leveraging NFs to circumvent historic obstructions of ExpM is a potentially transformational solution for differentially private ML worth attention. We introduce a new training method, ExpM+NF, as a potential alternative to DPSGD, and we provide experiment with logistic regression and a modern deep learning model to test whether training via ExpM+NF is viable with “good” privacy parameters. Under the assumption that the NF output distribution is the ExpM distribution, we are able to achieve  $\varepsilon$  as low as  $1e-3$ —three orders of magnitude stronger privacy with similar accuracy. This work outlines a new avenue for advancing differentially private ML, namely discovering NF approximation guarantees. Code to be provided after review.

<sup>\*</sup>Equal contribution <sup>1</sup>Oak Ridge National Laboratory, Oak Ridge, TN, USA. Correspondence to: Robert A. Bridges <[bridgesra@ornl.gov](mailto:bridgesra@ornl.gov)>, Vandy J. Tombs <[tombsvj@ornl.gov](mailto:tombsvj@ornl.gov)>.

Research sponsored by the Laboratory Directed Research and Development Program of Oak Ridge National Laboratory, managed by UT-Battelle, LLC, for the U. S. Department of Energy. This manuscript has been co-authored by UT-Battelle, LLC under Contract No. DE-AC05-00OR22725 with the US DOE. The United States Government retains and the publisher, by accepting the article for publication, acknowledges that the United States Government retains a non-exclusive, paid-up, irrevocable, world-wide license to publish or reproduce the published form of this manuscript, or allow others to do so, for United States Government purposes. The DOE will provide public access to these results of federally sponsored research in accordance with the DOE Public Access Plan (<http://energy.gov/downloads/doe-public-access-plan>).

Code containing experiments presented available at [redacted\\_URL](#).

Special thanks to Adam Spannaus and Vishakh Gopi for their wisdom with PyTorch and to Cory Watson for making sure the big computers “just work”.

*Under review for Proceedings of the 41<sup>st</sup> International Conference on Machine Learning, Vienna, Austria. PMLR 235, 2024. Copyright 2024 by the author(s).*

#### 1. Introduction

Differential privacy (DP) is the widely accepted standard for privacy preserving analytics and its adoption has extended into a variety of AI/ML applications (Xiong et al., 2014). Differentially private ML is currently achieved almost exclusively by a single, preeminent technique—Differentially Private Stochastic Gradient Descent (DPSGD) (Abadi et al., 2016; Ponomareva et al., 2023). DPSGD achieves a privacy guarantee by clipping and adding Gaussian noise to each gradient during SGD training, and upon the conclusion of training the many privacy guarantees (one per step) are collected into a single, overarching guarantee. Aiding DPSGD’s widespread adoption is 15 years of work on composition theorems (Dwork, 2007; 2010; Kairouz et al., 2017; Dong et al., 2021) which include methods that tighten the privacy bounds for mechanisms that utilize subsampling (e.g., ML training with batches) (Abadi et al., 2016; Mironov, 2017) and clever techniques that compose privacy curves using the privacy random variable (Gopi et al., 2021).

Despite these years of effort seeking to improve the privacy

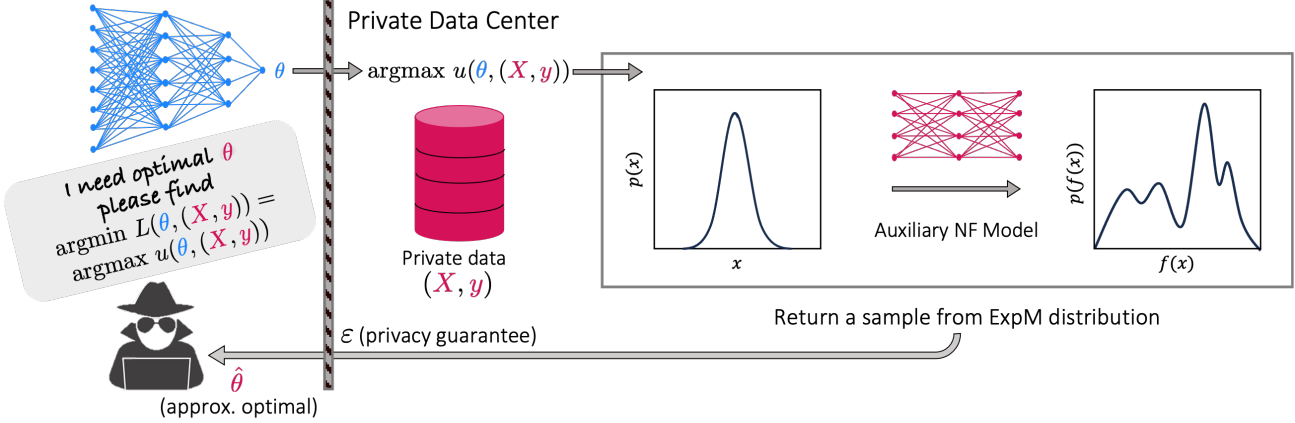


Figure 1: Figure depicts private data enclave on which outside entities would like to train a machine learning model. New technique, ExpM+NF, depicted at right, trains an auxiliary Normalizing Flow (NF) model to sample near optimal parameters from the otherwise intractable Exponential Mechanism (ExpM) density. Privacy parameters ( $\epsilon > 0, \delta = 0$ ) are pre-specified by the private data center.

bound for ML models trained with DPSGD, one can see in the conventional scenario of training ML on a single private dataset that DPSGD is wasteful by design. Privacy is expended so that all gradients may be publicized, yet all that is required is the trained model. This leads to the overall privacy guarantee worsening with each step during training, of which hundreds to tens of thousands are usually needed. Once the privacy budget is expended, training must cease, perhaps prematurely. This has led to an unusable accuracy-privacy tradeoff in practice (Kurakin, 2022; Suriyakumar et al., 2021). Secondly, by expending privacy at each gradient step, DPSGD can only provide *approximate* DP, i.e.,  $\delta > 0$  (see Definition 2.1), a consequence of relying on composition theorems and, independently, of using Gaussian noise.

In this paper, we advocate for a fundamentally different approach for achieving differentially private ML leveraging the Exponential Mechanism (ExpM) (McSherry & Talwar, 2007), a well-established DP technique for optimizing a utility (e.g., an inverse loss) function. The goal is to sample from the ExpM distribution, a probability distribution over the model’s parameter space (the domain of the utility/loss function) so that near-optimal (resp., far-from-optimal) parameters have high (resp., low) likelihood. By design, sampling from this distribution produces, with high likelihood, near-optimal parameters that are furnished with a strong privacy guarantee—pre-specified privacy  $\epsilon > 0$  and  $\delta = 0$ .

While ExpM is well known, two obstructions prevented its prior use in ML applications. First, an a priori bound on sensitivity must be proven for the given utility (equiv., loss) function, which is difficult in general, e.g., see (Minami et al., 2016). Secondly, sampling from the requisite distribution is intractable except for finite or otherwise very simple

sample domains, where ExpM reduces to sampling from a multinomial. Examples of using ExpM for differentially private ML in the finite setting exist, e.g.: (Friedman & Schuster, 2010) (private decision tree with only categorical features), (Kaprakov & Talwar, 2013) (private PCA), and (Vinterbo, 2012) (private feature selection with only categorical variables). Notwithstanding these examples, ExpM is historically intractable in most ML applications as the optimization is of a loss function over continuous parameter space (Kasiviswanathan et al., 2011; Ji et al., 2014; Minami et al., 2016; Near & Abuah, 2022).

For the first barrier, we constrain our training to  $\ell^2$  (equiv. MSE) loss, admitting a sensitivity bound for supervised learning tasks with bounded targets (accommodating classification tasks via binary/one-hot encoding)—Theorem 3.1. While we do not consider other loss functions, additional theorems for other loss functions could be developed and used in a similar manner, potentially with auxiliary privacy benefits.

To address the second obstruction, we leverage an auxiliary Normalizing Flow (NF) model—a deep learning model—that permits approximate sampling from the otherwise intractable ExpM density (Papamakarios et al., 2021). We note that other approximate sampling methods that leverage ML could prove just as promising. The combined technique, ExpM+NF (see Figure 1), promises a strong user-specified privacy guarantee ( $\epsilon > 0, \delta = 0$ ) with near optimal parameters. Further, by design ExpM+NF eliminates the iterative privacy loss observed in DPSGD.

Whether or not (and specifically how) one can train a desired ML model using ExpM+NF with ideally strong privacy parameter  $\epsilon$  is a research question. To justify this new ap-

proach, we implement experiments using ExpM+NF to train logistic regression (LR) and GRU-D, a deep learning model, on MIMIC-III data (Johnson et al., 2016). This exhibits that ExpM+NF can achieve the desired model performance. Assuming that the NF output is the ExpM density, our results show that ExpM+NF achieves similar accuracy with orders of magnitude better privacy (lower  $\varepsilon$  with  $\delta = 0$ ) than DPSGD. If the NF furnishes an accurate approximation of the ExpM distribution, then this method substantially improves the SOTA in differentially private ML.

We do not maintain that the privacy implications of the NF approximation can be ignored. Rather, our position is that *identifying strong bounds on NF approximation accuracy and their associated privacy guarantees now promises a route through the accuracy–privacy ceiling that currently constrains differentially private ML*. Such an advancement would prove transformational for differentially private ML; the vast increase in the privacy budget may be used to address other hardships, such as affording hundreds, possibly thousands of hyperparameter tuning runs (thereby increasing accuracy) while furnishing even better privacy.

## 2. Background

Here we introduce preliminary technical topics and leave a more thorough discussion of all background to Appendix A. Throughout, we denote the real numbers as  $\mathbb{R}$ ; the universe from which datasets  $X, X'$  are drawn as  $D$  (so  $X, X' \in D$ ); and use  $X, X'$  to denote neighboring datasets, meaning they are identical except for at most one data point (one row). The function  $u : \Theta \times D \rightarrow \mathbb{R}$  will be a utility or scoring function we wish to maximize privately over  $\Theta$ . In the setting of machine learning,  $\Theta$  is the space of parameters for an ML model  $\hat{y}$ , and we will denote a dataset from  $D$  as  $(X, Y)$  (features and targets, respectively) in lieu of simply  $X$ . Given loss function  $L(X, Y, \theta)$ , the utility is defined as  $u := \phi \circ L$ , with  $\phi$  strictly decreasing, and usually  $\phi(t) = -t$ . The term “mechanism” simply means random function. We use  $p$  for probability densities and capital  $P$  to denote the induced probability measure, i.e., for measurable set  $A$ ,  $P(A) := \int_A p(\theta) d\theta$ .

### 2.1. Differential Privacy

**Definition 2.1** (Differential Privacy). A mechanism  $f : \Theta \times D \rightarrow \mathbb{R}$  satisfies  $(\varepsilon, \delta)$ -Differential Privacy or is  $(\varepsilon, \delta)$ -DP if and only if

$$P(f(\theta, X) \in A) \leq P(f(\theta, X') \in A) e^\varepsilon + \delta$$

for all neighboring  $X, X' \in D$ ,  $\theta \in \Theta$ ,  $\varepsilon \geq 0$  and for all measurable sets  $A$ . When  $\delta = 0$ , we say  $f$  is  $\varepsilon$ -DP.

The  $\varepsilon$  term is an upper bound on the privacy loss. Approximate DP, or  $(\varepsilon, \delta)$ -DP, provides a relaxed definition— $\delta$

is the probability that the mechanism  $f$  is not guaranteed to be  $\varepsilon$ -DP. This “probability of failure” interpretation has led many to suggest that  $\delta$  should be no larger than  $1/|X|$  (Dwork & Roth, 2014).

To achieve differential privacy in practice, randomness is leveraged. Determining how much randomness to inject requires understanding how sensitive the output of the mechanism is across all neighboring datasets.

**Definition 2.2** (Sensitivity). The sensitivity of a mechanism  $f : \Theta \times D \rightarrow \mathbb{R}$  is  $\sup |f(\theta, X) - f(\theta, X')|$  where the supremum is over neighboring  $X, X' \in D$ , and all  $\theta \in \Theta$ . We use  $s$  to denote an upper bound on sensitivity.

**Definition 2.3** (Exponential Mechanism). For data  $X \in D$  and a utility function  $u : \Theta \times D \rightarrow \mathbb{R}$  with sensitivity  $s$ , the Exponential Mechanism (ExpM) returns  $\theta \in \Theta$  with likelihood  $p_{ExpM}(\theta; X) \propto \exp(\varepsilon u(\theta, X)/(2s))$ .

The following theorem shows ExpM satisfies  $\varepsilon$ -DP.

**Theorem 2.4** ((McSherry & Talwar, 2007; Dwork & Roth, 2014)). *The Exponential Mechanism (ExpM) i.e., sampling  $\theta \sim p_{ExpM}(\theta, X) \propto \exp(\varepsilon u(\theta, X)/(2s))$  where utility function  $u$  has sensitivity  $s$ , provides  $\varepsilon$ -DP.*

The original treatment of ExpM (McSherry & Talwar, 2007) furnishes utility theorems—rigorous guarantees that bound how far ExpM samples can be from the optima.

### 2.2. Normalizing Flows (NFs)

We reference readers to the survey of NF research by Papamakarios et al. (Papamakarios et al., 2021). An NF model is a neural network,  $g = g_k \circ \dots \circ g_1 : \mathbb{R}_z^n \rightarrow \mathbb{R}_\theta^n$ , with each layer  $g_i : \mathbb{R}^n \rightarrow \mathbb{R}^n$ , called a flow, that is invertible and differentiable. We let  $\theta_{NF}$  denote the parameters of  $g$  to be learned, and suppress this notation for simplicity unless needed. Notably,  $g$  (and by symmetry,  $g^{-1}$ ) preserves probability densities: if  $p_z$  is a probability density, then  $\theta \mapsto p_z(g^{-1}(\theta))|\det J_{g^{-1}}(\theta)|$  is also, which is proven by the change of variables induced by  $\theta = g(z)$ .

Let  $p_\theta^*$  be an intractable target density over  $\mathbb{R}^n$  (meaning  $p_\theta^*$  can be computed up to a constant factor, but we cannot sample from  $p_\theta^*$ ), in our case  $p_\theta^* = p_{ExpM}$ . Let  $p_z$  be a tractable density over  $\mathbb{R}^n$ , esp.,  $p_z$  is Gaussian. Then  $g$  can be trained to transform  $p_z$  into  $p_\theta$  so that  $p_\theta \approx p_\theta^*$  as follows: iteratively sample a batch  $z_i \sim p_z, i = 1, \dots, N$  and minimize the empirical KL divergence of the base density  $p_z$  with the pull-back of the target density, namely  $p_\theta^*(g(z))|\det J_g(z)|$ . This is “Reverse KL” (RKL) loss, which we approximate with a monte carlo estimate,

$$KL[p_z(z) \parallel p_\theta^*(g(z))|\det J_g(z)|] \approx$$

$$\frac{1}{N} \sum_{i=1}^N \log \frac{p_z(z_i)}{p_\theta^*(g(z_i))|\det J_g(z_i)|}.$$

In practice our loss function neglects terms that do not include parameters of  $g$  as they do not affect training; in particular,  $p_\theta^* = \exp(f(\theta))/Z$ , and we only include the log of the numerator,  $\log[p_\theta^* Z] = \log[\exp(f)] = f$ , thereby avoiding computation of the normalization constant  $Z$ :

$$\mathcal{L} = -\frac{1}{N} \sum_{i=1}^N \log[p_\theta^*(g(z_i))Z] + \log|\det J_g(z_i)| \quad (1)$$

Once trained,  $\theta = g(z)$  with  $z \sim p_z$  gives approximate samples from previously intractable  $p_\theta$ !

In the ExpM setting  $\log(p_\theta^*(\theta_i)Z) = u(\theta_i, X, Y)\varepsilon/(2s)$ , so performant computation of the utility function is required. Generally, NFs are designed to make computing the log determinant term computationally feasible (e.g., using flows  $g_i$  so that  $J_g$  is triangular or that satisfy Theorem B.2) while balancing the expressiveness. In this work, we leverage the Planar Flows of Rezende & Mohamed (Rezende & Mohamed, 2015) and their more expressive generalization, Sylvester Flows (Van Den Berg et al., 2018).

#### Algorithm 1 Differentially Private ML with Exp+NF

**Input:** Training set  $(X, Y)$ , a base distribution  $p_z$ , a loss function  $L$ , decreasing  $\phi$ , privacy budget  $\varepsilon$ , sensitivity bound  $s$ , epochs  $T$ .  
**Initialize**  $\theta_{\text{NF},0}$  randomly  
**for**  $t$  in  $[T]$  {Train Auxiliary NF Model} **do**  
     **Generate  $N$  samples from base distribution**  
      $z_i \sim p_z$   
     **Produce  $N$  parameter samples & Jacobian**  
      $\theta_i = g_{\theta_{\text{NF},t}}(z_i)$   
      $\log |\det J_g(z_i)|$  (depends on NF)  
     **Compute utility for each parameter sample**  
     for each  $i \in [N]$ ,  $u(X, Y, \theta_i) = \phi \circ L(X, Y, \theta_i)$   
     **Evaluate target log likelihood (up to a constant)**  
      $\log[p_\theta^*(\{\theta_i\})Z] = \frac{\varepsilon}{2s} \sum_{i=1}^N u(X, Y, \theta_i)$   
     **Compute Reverse KL Loss using Eq. 1**  
      $\mathcal{L} = KL[p_z(z_i) \parallel p_\theta^*(\theta_i)|\det J_g(z_i)|] + C$   
     **Update NF Model**  
      $\theta_{\text{NF},t+1} = \theta_{\text{NF},t} - \eta_t \nabla_{\theta_{\text{NF},t}} \mathcal{L}$   
**end for**  
     sample from base distribution,  $z \sim p_z$   
**Output** Model parameters,  $\theta = g_{\theta_{\text{NF},T}}(z)$ , privacy  $\varepsilon$

### 3. ExpM+NF Method

Figure 1 describes the setting that we will consider: a private data enclave that wishes to permit optimization on their data; in particular, training and publicly releasing an ML algorithm on that data. The basic method for producing a differentially private ML model with ExpM+NF is given in Algorithm 1.

Fitting an ML model on training features and targets  $(X, Y)$  constitutes finding parameters  $\theta$  that minimizes a loss function  $L(X, Y, \theta)$ , ExpM requires specifying a utility function  $u(X, Y, \theta)$  to be maximized in  $\theta$ ; thus,  $u = \phi \circ L$  for strictly decreasing  $\phi$ . Throughout, we will consider  $u = -L$ .<sup>1</sup> To define the ExpM density, we must provide  $s$ , a bound on  $u$ 's sensitivity (Defn. 2.2).<sup>2</sup> In this initial work, we consider  $\ell^2$  loss functions ( $\sum_{X,Y} (\hat{y}(x) - y)^2$ ) on classification tasks with model outputs and targets bounded by 1. Here we show these conditions give  $s = 1$ .

Define the utility to be the negative loss so

$$u = -L = \sum_{(x,y) \in (X,Y)} l(x, y, \theta) + r(\theta)$$

where  $l(x, y, \theta)$  is the loss from data point  $(x, y)$ , and  $r(\theta)$  is a regularization function. For two neighboring datasets  $(X, Y), (X', Y')$ , let  $(x, y) \in (X, Y)$  and  $(x', y') \in (X', Y')$  denote the lone row of values that are not equal. We obtain  $|u(X, Y, \theta) - u(X', Y', \theta)| = |l(x, y, \theta) - l(x', y', \theta)|$  (all terms of  $L$  cancel except that of the differing data point); hence, bounding  $s$  is achieved by Lipschitz or  $\ell^\infty$  conditions on the per-data-point loss function  $l$ . Regularization  $r$  does not affect sensitivity.

**Theorem 3.1** (Sensitivity bound for  $\ell^2$  loss). *Suppose our targets and model outputs reside in  $[0, 1]$ . If  $u = -L = -\sum_{(x,y)} (\hat{y}(x, \theta) - y)^2$ , then  $s \leq 1$ .*

*Proof.* Since  $\hat{y}(x, \theta), y \in [0, 1]$  we see  $(\hat{y}(x, \theta) - y)^2 \in [0, 1]$  and  $(\hat{y}(x, \theta) - y')^2 \in [0, 1]$  so  $|u(X, Y, \theta) - u(X', Y', \theta)| = |(\hat{y}(x, \theta) - y)^2 - (\hat{y}(x', \theta) - y')^2| \leq 1$ .  $\square$

**Corollary 3.2.** *Sensitivity  $s \leq 1$  for classification tasks using binary/one-hot encoded targets and logistic/soft-max outputs with  $\ell^2$  loss and  $u = -L$ .*

Near optimal  $\theta$  are found by sampling  $\theta \sim p_{\text{ExpM}}(\theta) \propto \exp[u(X, Y, \theta)\varepsilon/2s]$  equipped with a pre-specified  $\varepsilon$ -DP guarantee. This step replaces an SGD scheme but fills the same role—it produces approximately optimal parameters for the ML model. Unfortunately,  $p_{\text{ExpM}}$  is a historically

<sup>1</sup>While any strictly decreasing  $\phi$  theoretically ensures identical optimization, in practice  $\phi$  must separate the near-optimal  $\theta$  from those that are far from optimal. This means the derivative must be a sufficiently large negative value over an appropriate range of  $L(\theta)$  to discriminate high versus low utility  $\theta$ . In particular, using a negative sigmoid function, which is flat ( $\phi' \approx 0$ ) except in a limited neighborhood, is unwise, unless we know which range of  $L(\theta)$  will contain the optimal values a priori and shift  $\phi$  to discriminate these values. Lastly, we note that choice of  $\phi$  effects the sensitivity, and therefore may be designed to assist in producing the required sensitivity bound.

<sup>2</sup>When  $s$  is large, it diminishes influence of  $u$  and reduces accuracy by increasing the variance of  $\theta$ . Since  $u, s$  are intimately tied to the loss function  $L$ , bounding  $s$  is generally required per loss function and can depend on the model outputs.

intractable density for non-finite domains, so sampling directly is infeasible in most supervised learning applications. Our approach trains an auxiliary NF model (Section 2.2) to transform a Gaussian base density  $p_z$  into our target density  $p_\theta^* := p_{ExpM} \propto \exp(u\varepsilon/(2s))$ . The NF training (Section 2.2) is computationally well suited for approximating the ExpM density. The Reverse KL loss function (Eq. 1) only requires computing the determinant Jacobian (made tractable by the design of the NF) and  $\log[p_\theta^*(\theta)Z] = u\varepsilon/(2s)$ , essentially our loss function. Finally, supposing the NF output density is a good approximation of the ExpM density, a sample from the NF can be released with the  $\varepsilon$ -DP guarantee.

## 4. Examining ExpM+NF Potential on MIMIC-III

The previous section outlines a new method for obtaining optimal parameters for an ML model, yet it is unclear if sampling parameters from an NF model can produce an accurate ML model especially, when ideally small  $\varepsilon$  are used. To test the feasibility and show the promise of ExpM+NF method, we provide experimental results by training a logistic regression (LR) and a deep learning model (GRU-D) on MIMIC-III—a large, open, electronic health record database covering a diverse group of critical care patients at a medical center from 2001–2012. We use the binary prediction task benchmarks ICU Mortality and ICU Length of Stay ( $> 3$  days) from Wang et al. (Wang et al., 2020). Results of non-private LR and GRU-D (Che et al., 2018) models are provided by Wang et al. and Suriyakumar et al. (Suriyakumar et al., 2021) provide DPSGD (with RDP accountant) results on these tasks as well. To the best of our knowledge, Suriyakumar et al. (Suriyakumar et al., 2021) present the state of the art in differentially private ML on these MIMIC-III benchmarks. Unfortunately, their code is not provided.

We replicate these benchmarks as closely as possible. For all tasks and models (LR and GRU-D) we implement a non-private baseline, DPSGD and ExpM+NF trained private versions. ExpM+NF is currently constrained to using  $\ell^2$  loss (needed for the sensitivity bound). For the non-private and DPSGD models, we provide results for both binary cross entropy loss (BCE) and  $\ell^2$  loss, as both are common for binary classification. For privacy methods, we vary  $\varepsilon$  to see the accuracy-privacy tradeoff. Differentially private ML research generally considers  $\varepsilon \in [1, 10]$  (Ponomareva et al., 2023), hence we present plots of  $0.5 \leq \varepsilon \leq 10$ , and, investigate results for  $\varepsilon$  as low as  $1e-4$ . All experiments are coded in PyTorch.

For each  $\varepsilon$ , we performed a randomized grid search of hyperparameters fitting on the train set and evaluating on the dev (development, or validation set) set. For DPSGD, we use the PRV method of accounting via Opacus (Yousefpour

et al.; 2021). Our NF models always use a Gaussian base distribution with  $N(\vec{0}, \text{diag}(\sigma^2))$ , and we treat the constant  $\sigma^2$  appearing on the diagonal of the covariance matrix as a hyperparameter. We use AUC as our accuracy metric as the task is binary classification. Starting conditions can lead to anomalously good/bad models for all methods (non-private, DPSGD, ExpM+NF) so we present the median across ten models evaluated on the hold out test set, each with different random seeds, to provide robustness to outliers.

Further experimental set up details, including more information on the MIMIC-III dataset and benchmarks, how we performed the hyperparameter search, and how we present the results as the median across ten models, are in the Appendix C.

### 4.1. Accuracy-Privacy Results

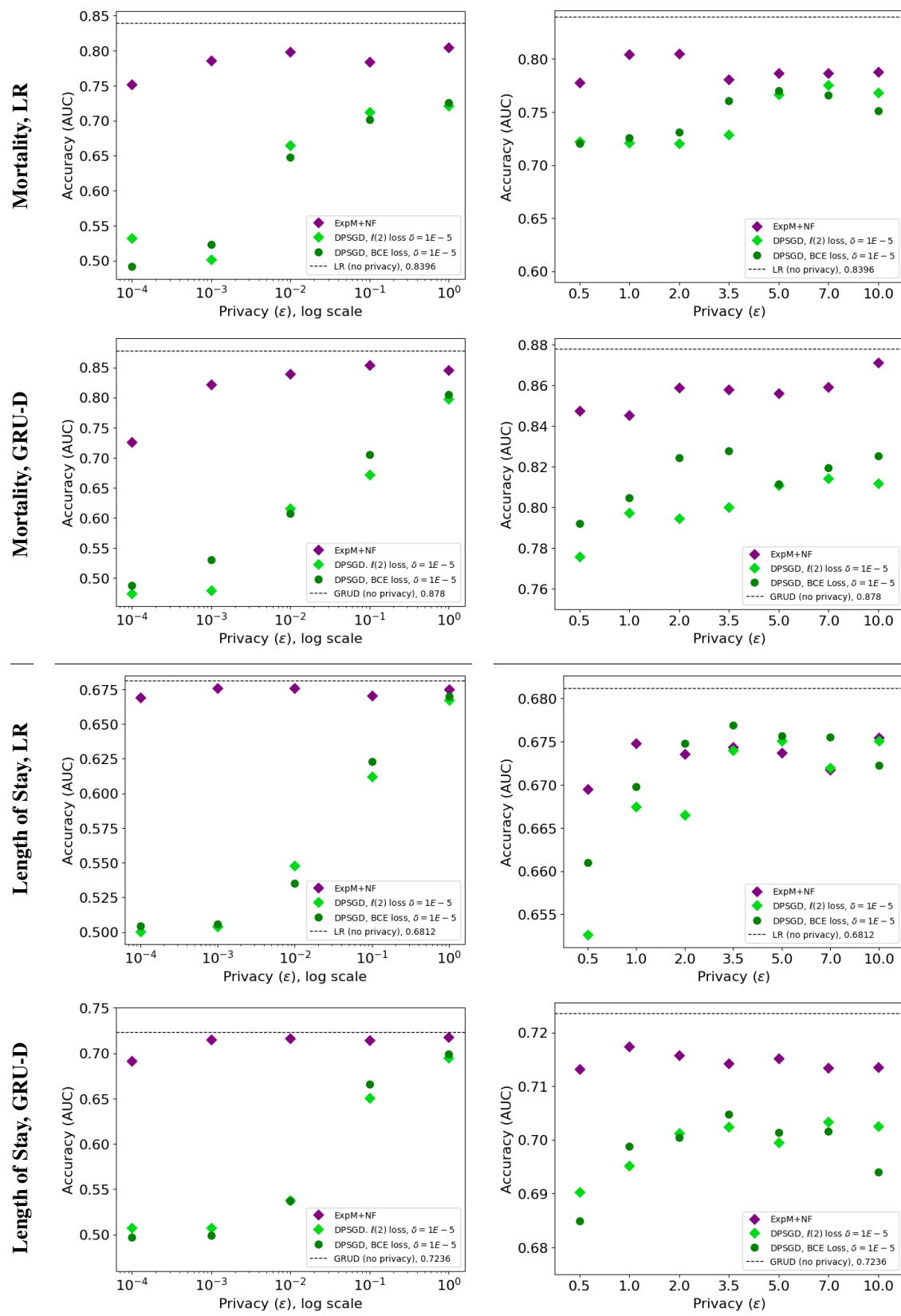
As our goal is to test if ExpM+NF is a viable training method, our results report accuracy (AUC) versus privacy ( $\varepsilon$ ), assuming the sampling from the trained NF is the exponential mechanism. Under this assumption, our overall finding is that ExpM+NF substantially outperforms (our now state-of-the-art) DPSGD results in accuracy and privacy. Table 1 displays accuracy-versus-privacy results. In every experiment, ExpM+NF exhibits greater than 94% of the non-private models’ AUC for all  $\varepsilon \geq 1e-3$ . ExpM+NF surpasses DPSGD in all experiments except  $\varepsilon \geq 2$  with LR model on the Length of Stay task, in which all privacy methods achieve 99% of the non-private model’s AUC. Viewed through another lens, ExpM+NF maintains a greater AUC for  $\varepsilon \geq 1e-3$  than DPSGD for  $\varepsilon = 1, \delta = 1e-5$  in all MIMIC-III experiments, respectively. For both prediction tasks, the AUCs achieved by ExpM+NF of the GRU-D model are, for all  $\varepsilon \geq 1e-3$ , better than the non-private LR or GRU-D models’ results reported by Suriyakumar (Suriyakumar et al., 2021). These results show that ExpM+NF is a viable training method even for  $\varepsilon$  values orders of magnitude smaller (orders of magnitude better privacy) than is currently considered.

Appendix D provides many other findings including investigation of the NF distributions and ancillary results showing our DPSGD implementations push the previous state of the art for these MIMIC-III benchmarks.

### 4.2. Timing Results

Another aspect to the viability of this method is its impact on the training time performance (as it requires training an auxiliary NF model). Here we present timing results for ICU Mortality experiments in Table 2. Timing results for Length of Stay are similar and reside in Appendix D.3 along with more details of this timing experiment. All private training methods are slower than non-private (expected), and that when including the time to compute the

Table 1: Median AUC results on MIMIC-III Mortality and Length of Stay prediction experiments



noise\_multiplier, DPSGD is slower than ExpM+NF for both LR and GRU-D training. The innovation here is that our ExpM+NF code computes (and tracks gradients through) the  $\ell^2$  loss for the sampled parameters  $\theta_i$  in parallel when computing the RKL loss for training the NF, rather than computing this sequentially. We used the best hyperparameters for each model,  $\varepsilon$ , so batch size and epochs vary between the different implementations and privacy levels.

## 5. Conclusion & Future Research

The fundamental observation driving this new direction is that differentially private ML is constrained by an accuracy-privacy tradeoff that is often unusable in practice. Examining DPSGD, the de facto method for differentially private ML, we find that the algorithm is wasteful by design in all but the singular scenario when gradients are to be made public—noise is added to every gradient diminishing privacy with each epoch, and this entails the need for advanced composition theorems ensuring that  $\delta > 0$ . Our critical insight is two-fold: first, the well-established ExpM provides a tailored solution that bypasses these two problems, but the requisite distribution for ML applications is intractable; second, NF models provide a promising avenue for sampling from the ExpM distribution.

As we explored this new approach, we found that ExpM+NF exhibits similar, often greater accuracy than DPSGD when using orders of magnitude smaller privacy parameter ( $\varepsilon$ ), and is computationally similar. *In short, ExpM+NF is a viable training method, and has the potential to be transformational for the field of differentially private ML.* In all DP applications, randomness is produced from some approximation algorithm (and often privacy guarantees follow from the assumption of true randomness); e.g., DPSGD uses psuedo-random Gaussian samples in practice, and ExpM+NF uses samples from the NF output distribution. We do not argue that these are equivalent, nor that the NF approximation’s effect on privacy can be ignored; rather we argue that mathematical guarantees of the NF’s approximation abilities are a gateway to breaking through the current accuracy-privacy impasse constraining the field of differentially private ML.

*This leads to a very clear next-step: analyzing the approximation ability of the NFs in this setting and its impact on privacy.* For any (private) training data sets  $X$ , let  $p_X$  denote the the ExpM+NF output density, and  $p_X^*$  the ExpM (target) density satisfying  $\varepsilon_1$ -DP. Supposing for the moment, one can attain the results  $\|1 - p_X/p_X^*\|_\infty < \varepsilon_2$ , then we see  $\log(p_X/p_X^*) = \log(p_X/p_X^*) + \log(p_X^*/p_X^*) + \log(p_X^*/p_X) < 2\varepsilon_2 + \varepsilon_1$  since  $\log(t) \leq t - 1$ . Hence, rigorous privacy guarantees of ExpM+NF follow immediately. Notably emerging works are investigating the mathematical guarantees of NFs approximation abilities (Kong & Chaudhuri, 2020; Lu & Lu, 2020; Verine et al., 2023). Other

avenues to such a result may exist.

The promise of vastly improved accuracy-privacy trade-off would allow simple solutions to some of the difficulties that occur when training with differential privacy. For example, hyperparameter optimization is often needed to find the best model, yet it incurs a privacy cost that could be budgeted.

In this work, bounding the sensitivity of the loss function, as is required for ExpM, was done by using  $\ell^2$  loss and the fact that our targets were bounded (binary, or one-hot). Moving to a more general setting, especially regression with  $\ell^2$  loss or classification with other prominent loss functions, esp. log loss and KL divergence loss, will require custom sensitivity bounds for ExpM+NF (e.g., see (Minami et al., 2016)). Our results show that non-private and DPSGD training had similar results for both BCE and  $\ell^2$  loss in these classification tasks; on the other hand, the choice of loss function may prove a bigger effect on ExpM+NF’s results since the sensitivity bounds has a direct effect on the variance of ExpM distribution.

While this concludes our paper, we hope it is the start of many fruitful follow-on investigations and sparks change in the set of possibilities under consideration for advancing differentially private ML.

## References

Abadi, M. et al. Deep learning with differential privacy. In *Proceedings of the 2016 ACM SIGSAC conference on computer and communications security*, 2016.

Che, Z. et al. Recurrent neural networks for multivariate time series with missing values. *Scientific reports*, 8(1): 1–12, 2018.

Dong, J., Roth, A., and Su, W. Gaussian differential privacy. *Journal of the Royal Statistical Society*, 2021. URL <https://par.nsf.gov/biblio/10215709>.

Dwork, C. Sequential composition of differential privacy. *Theory of Cryptography*, pp. 222–232, 2007.

Dwork, C. Advanced composition of differential privacy. In *Proceedings of the 41st Annual ACM Symposium on Theory of Computing*, pp. 436–445, 2010.

Dwork, C. and Roth, A. The algorithmic foundations of differential privacy. *Found. Trends Theor. Comput. Sci.*, 9(3-4):211–407, 2014.

Friedman, A. and Schuster, A. Data mining with differential privacy. In *Proceedings of the 16th ACM SIGKDD international conference on Knowledge discovery and data mining*, pp. 493–502, 2010.

Gopi, S., Lee, Y. T., and Wutschitz, L. Numerical composition of differential privacy. In Ranzato, M., Beygelzimer,

Table 2: ICU Mortality Mean Benchmark Timing Results

Training	Loss	Logistic Regression			GRU-D		
		Training Time	Computing $\varepsilon$	Total	Training Time	Computing $\varepsilon$	Total
Non- Private	$\ell^2$	.87 ms	—	.87 ms	.84 ms	—	.84 ms
	BCE	1.67 ms	—	1.67 ms	.93 ms	—	.93 ms
DPSGD	$\ell^2$	1.16 ms	1.13 ms	2.29 ms	1.38 ms	1.44 ms	2.82 ms
	BCE	1.56 ms	1.2 ms	2.76 ms	1.46 ms	1.34 ms	2.8 ms
ExpM+NF	RKL+ $\ell^2$	1.65 ms	—	1.65 ms	1.71 ms	—	1.71 ms

A., Dauphin, Y., Liang, P., and Vaughan, J. W. (eds.), *Advances in Neural Information Processing Systems*, volume 34, pp. 11631–11642. Curran Associates, Inc., 2021. URL [https://proceedings.neurips.cc/paper\\_files/paper/2021/file/6097d8f3714205740f30debe1166744e-Paper.pdf](https://proceedings.neurips.cc/paper_files/paper/2021/file/6097d8f3714205740f30debe1166744e-Paper.pdf).

Ji, Z., Lipton, Z. C., and Elkan, C. Differential privacy and machine learning: a survey and review. *arXiv preprint arXiv:1412.7584*, 2014.

Johnson, A. E. W. et al. MIMIC-III, a freely accessible critical care database. *Scientific data*, 3, 2016.

Kairouz, P., Oh, S., and Viswanath, P. The composition theorem for differential privacy. *IEEE Transactions on Information Theory*, 63(6):4037–4049, 2017.

Kapralov, M. and Talwar, K. On differentially private low rank approximation. In *Proceedings of the twenty-fourth annual ACM-SIAM symposium on Discrete algorithms*, pp. 1395–1414. SIAM, 2013.

Kasiviswanathan, S. P., Lee, H. K., Nissim, K., Raskhodnikova, S., and Smith, A. What can we learn privately? *SIAM Journal on Computing*, 40(3):793–826, 2011. URL <https://doi.org/10.1137/090756090>.

Kong, Z. and Chaudhuri, K. The expressive power of a class of normalizing flow models. In *International conference on artificial intelligence and statistics*, pp. 3599–3609. PMLR, 2020.

Kurakin, A. Applying differential privacy to large scale image classification, 2022. URL <https://ai.googleblog.com/2022/02/applying-differential-privacy-to-large.html>. Accessed: 2023-07-25.

Lu, Y. and Lu, J. A universal approximation theorem of deep neural networks for expressing probability distributions. *Advances in neural information processing systems*, 33: 3094–3105, 2020.

McSherry, F. and Talwar, K. Mechanism design via differential privacy. In *IEEE Symposium on Foundations of Computer Science*, pp. 94–103, 2007. doi: 10.1109/FOCS.2007.66.

Minami, K., Arai, H., Sato, I., and Nakagawa, H. Differential privacy without sensitivity. In *Advances in Neural Information Processing Systems* 29, 2016.

Mironov, I. Rényi differential privacy. In *2017 IEEE 30th computer security foundations symposium (CSF)*, pp. 263–275. IEEE, 2017.

Near, J. P. and Abuah, C. Programming differential privacy, 2022. URL <https://programming-dp.com/>. Accessed: 2023-09-15.

Papamakarios, G. et al. Normalizing flows for probabilistic modeling and inference. *Journal of Machine Learning Research*, 22(57):1–64, 2021.

Pedregosa, F., Varoquaux, G., Gramfort, A., Michel, V., Thirion, B., Grisel, O., Blondel, M., Prettenhofer, P., Weiss, R., Dubourg, V., Vanderplas, J., Passos, A., Cournapeau, D., Brucher, M., Perrot, M., and Duchesnay, E. Scikit-learn: Machine learning in Python. *Journal of Machine Learning Research*, 12:2825–2830, 2011.

Ponomareva, N., Hazimeh, H., Kurakin, A., Xu, Z., Denison, C., McMahan, H. B., Vassilvitskii, S., Chien, S., and Thakurta, A. G. How to dp-fy ML: a practical guide to machine learning with differential privacy. volume 77, pp. 1113–1201, 2023.

Rezende, D. and Mohamed, S. Variational inference with normalizing flows. In *International Conference on Machine Learning*, 2015.

Sun, X. and Bischof, C. A basis-kernel representation of orthogonal matrices. *SIAM journal on matrix analysis and applications*, 16(4):1184–1196, 1995.

Suriyakumar, V. M., Papernot, N., Goldenberg, A., and Ghassemi, M. Chasing your long tails: Differentially private prediction in health care settings. In *Proceedings of*

the 2021 ACM Conference on Fairness, Accountability, and Transparency, pp. 723–734, 2021.

Van Den Berg, R. et al. Sylvester normalizing flows for variational inference. In 34th Conference on Uncertainty in Artificial Intelligence, 2018.

Verine, A., Negrevergne, B., Chevaleyre, Y., and Rossi, F. On the expressivity of bi-lipschitz normalizing flows. In Khan, E. and Gonen, M. (eds.), Proceedings of The 14th Asian Conference on Machine Learning, volume 189 of Proceedings of Machine Learning Research, pp. 1054–1069. PMLR, 12–14 Dec 2023. URL <https://proceedings.mlr.press/v189/verine23a.html>.

Vinterbo, S. A. Differentially private projected histograms: Construction and use for prediction. In Joint European Conference on Machine Learning and Knowledge Discovery in Databases, pp. 19–34. Springer, 2012.

Wang, S. et al. MIMIC-extract github repository. URL [https://github.com/MLforHealth/MIMIC\\_Extract](https://github.com/MLforHealth/MIMIC_Extract). Accessed: 2023-05-25.

Wang, S. et al. Mimic-extract: A data extraction, preprocessing, and representation pipeline for mimic-iii. In Proceedings of the ACM conference on health, inference, and learning, 2020. URL [https://github.com/MLforHealth/MIMIC\\_Extract](https://github.com/MLforHealth/MIMIC_Extract).

Xiong, P., Zhu, T.-Q., and Wang, X.-F. A survey on differential privacy and applications. Jisuanji Xuebao/Chinese Journal of Computers, 37(1):101–122, 2014.

Yousefpour, A., Shilov, I., Sablayrolles, A., et al. Opacus: User-friendly differential privacy library in PyTorch. In NeurIPS Workshop Privacy in Machine Learning, 2021.

Yousefpour, A. et al. Codebase Opacus. <https://opacus.ai/>. Accessed: 2023-07-25.

## A. Further Background on Differential Privacy

Intuitively, differential privacy measures how much an individual data point changes the output distribution of the mechanism  $f$ . If the mechanism's output is nearly identical in both cases (when any data point is or isn't included), meaning that  $\varepsilon$  is very small, then this is a privacy guarantee for any individual data point. This quantifies the intuitive notion that it is essentially indistinguishable if any one data point is included or not.

Differential privacy has many useful properties. First, post-processing is “free”, meaning if  $f(\theta, X)$  is  $(\varepsilon, \delta)$ -DP, the same guarantee holds after composition with any function  $h$ ; i.e.,  $h \circ f$  is also  $(\varepsilon, \delta)$ -DP (Dwork & Roth, 2014). Secondly, it satisfies composition theorems; the most basic of which says that if  $f_1$  and  $f_2$  satisfy  $(\varepsilon_1, \delta_1)$ -DP and  $(\varepsilon_2, \delta_2)$ -DP, respectively, then  $f_1 \circ f_2$  satisfies  $(\varepsilon_1 + \varepsilon_2, \delta_1 + \delta_2)$ -DP (Dwork & Roth, 2014). The general problem of estimating the overall privacy bound (a single  $(\varepsilon, \delta)$ ) for a sequence of mechanisms  $f_i(\theta_i, X), i = 1, \dots, m$  each furnished with a privacy guarantee  $(\varepsilon_i, \delta_i)$ -DP, is important for use.

As the basic composition theorem above holds, it is not a tight bound (better estimates may exist), and hence, a large body of work (Dwork, 2007; 2010; Kairouz et al., 2017; Abadi et al., 2016; Dong et al., 2021; Gopi et al., 2021) provide advanced composition theorems (tradeoffs of  $\varepsilon$  and  $\delta$  that depend on the  $\varepsilon_i, \delta_i$ ) that estimate this overall bound. Intuitively, as more information is released (as  $m$  grows), the overall privacy guarantee gets worse ( $\varepsilon$  and  $\delta$  increase), and all advanced composition theorems entail an increase of  $\delta$  for the better estimate of  $\varepsilon$ .

## B. Further Background on Normalizing Flows

Let  $z \in \mathbb{R}^d$ ,  $A \in \mathbb{R}^{d \times m}$ ,  $B \in \mathbb{R}^{m \times d}$ ,  $c \in \mathbb{R}^m$ , and  $h : \mathbb{R} \rightarrow \mathbb{R}$  an activation function that we ambiguously apply to vectors componentwise ( $h(\vec{v}) = [h(v_1), \dots, h(v_d)]^t$ ).

**Definition B.1** (Sylvester Flow). A Sylvester flow is defined as  $g(z) = z + Ah(Bz + c)$ , and note that  $J_g(z) = I_d + A_{d \times m} \text{diag}(h'(Bz + c))_{m \times m} B_{m \times d}$ .

**Theorem B.2** (Sylvester a.k.a. Weinstein–Aronszajn Theorem).  $\det(I_d + A_{d \times m} B_{m \times d}) = \det(I_m + B_{m \times d} A_{d \times m})$ .

It follows that when  $m < d$ , we can compute the determinant,  $J_g(z)$  in the lower dimensional representation!

**Definition B.3** (Planar Flow). A planar flow is a special case of a Sylvester flow when  $m = 1$ , so  $A, B \in \mathbb{R}^d$ .

Following Berg et al. (Van Den Berg et al., 2018), a Sylvester Flow can be implemented by using the special case where  $A = Q_{d \times d} R_{d \times m}$  and  $B = \hat{R}_{m \times d} Q_{d \times d}^t$  with  $Q$  orthogonal and  $R, \hat{R}$  upper triangular. (This is a restriction in that it uses the same  $Q$  for both  $A, B$ ). To instantiate an orthogonal matrix  $Q$ , we define unit vectors  $v$  and set  $Q := \prod_v I - 2vv^t$  which is a product of Householder reflections. A well known fact is that Householder reflections are orthogonal, and any orthogonal matrix is as a product of Householder reflections (Sun & Bischof, 1995). Note this is obviated in the Planar Flow case since  $A, B$  are simply  $d$ -dimensional vectors.

## C. Experiment Details

For DPSGD we use PRV accounting we use clipping parameter, `max_grad_norm = 1` (Yousefpour et al., 2021),  $\delta = 1e-5$ , roughly the inverse of the number of training data points, as are standard, and `delta_error` set to  $\delta/1000$  (default). We compute the `noise_multiplier` parameter, which governs the variance of the Gaussian noise added to each gradient, to achieve the target privacy  $(\varepsilon, \delta)$  based on the number of gradient steps (`epochs` and `batch_size` parameters) and the gradient clipping parameter `max_grad_norm`. The PRV Accounting method introduces an error term for  $\varepsilon$  that bounds the error in the estimate of the privacy guarantee. Notably, `eps_error = .01` is the default fidelity, and computations become too expensive or intractable for `eps_error < .0001`. Hence, given target  $\varepsilon$ , we set `eps_error` to be as close as possible to  $\bar{\varepsilon}/100$  within the range [.0001, .01].

Data is split into a train/development (dev)/test split that is stratified, preserving class bias in each partition. For each  $\varepsilon$ , we performed a randomized grid search of hyperparameters fitting on the train set and testing on the dev set. The hyperparameters were refined usually twice for a total of about 60-90 hyperparameter train/dev runs; this same procedure is used for all training methods (ExpM+NF, DPSGD, non-private). Only those hyperparameters producing the best results on the dev set are used in final results—fitting on training plus dev partitions and validating on the never-before-used test set. While in practice, hyperparameter searching will entail a loss of privacy, we ignore accounting for this as our goal is to compare the best achievable accuracy and privacy of ExpM+NF, DPSGD, relative to the nonprivate baseline.

For DPSGD, the usual hyperparameters (epochs, batch size, momentum, learning rate, and regularization parameter) function as usual. For the NF models, the number of flows and parameters of the Sylvester model (Sec. 2.2, B) are also hyperparameters. Lastly, our method has hyperparameters for training that include: epochs, NF batch size (how many model parameters to sample from the NF for each KL loss computation), data batch size (number of training data points used in each KL loss computation), learning rate, momentum, and regularization parameter.

While batch normalization is commonplace in non-private deep learning, it is not directly portable to the private setting as  $z$ -normalization learned in training must be shipped with the model (Yousefpour et al., 2021); hence, we do not use batch normalization for our private models, but we do provide results with vs. without batch normalization where applicable, namely for the non-private GRU-D model, Table 4. Details of the hyperparameters used for each model can be found in our code base and vary per experiment and privacy level  $\varepsilon$ .

To address anomalous starting conditions, for both DPSGD and non-private training with BCE and  $\ell^2$  loss, once hyperparameter searching is complete, we train ten non-private baseline models, each with a different random seed, and present the median AUC. The highest non-private median across the two loss functions is the considered the baseline for each dataset, task and appears as a dotted line in result plots. For ExpM+NF we train ten NFs using the best hyperparameters and produce 1,000 sampled parameter sets from each NF, for a total of 10,000 parameter sets. We instantiate the 10,000 resulting models, compute their AUC results, and compare the median to DPSGD and the non-private baseline. One may prefer to compute the median of the 1,000 AUCs per NF model (producing 10 median AUCs), and report the median of these medians. We have empirically verified that the results are nearly identical in our experiments.

### C.1. MIMIC-III Details

Our experimental design follows a progression of research on MIMIC-III. Wang et al. (Wang et al., 2020) create benchmarks of needed healthcare predictive tasks from the MIMIC-III dataset, downloadable (from MIMIC-III v1.4, as `all_hourly_data.h5`) with the codebase (Wang et al.). We use the binary prediction task benchmarks ICU Mortality and ICU Length of Stay ( $> 3$  days) from Wang et al.’s pipeline. These tasks differ only in target and share the feature set consisting of 104 measurement means per hour over a 24 hour period for 21,877 patients. Mortality is very imbalanced (07.4%/92.6%), while Length of Stay is balanced (47.1%/52.9%). We employ standardization ( $z$ -score normalization) for each feature, and it is applied independently per train/dev/test partition to prevent privacy issues.

As an example use of the ICU Mortality and Length of Stay benchmarks, Wang et al. also present results of non-private LR and GRU-D (Che et al., 2018) models. Che et al. (Che et al., 2018) introduce the Gated Recurrent Unit with Decay (GRU-D) model, a deep neural network for time series learning tasks. GRU-D interpolates between the last seen value and the global mean so censored (missing) data does not need to be imputed in advance. Additionally, the hidden units of the GRU are decayed to zero with learned decay per component, which allows features that should have short influence (e.g., heart rate) vs. long influence (e.g., dosage/treatment) to have learned rate of diminishing value. Wang et al. provide non-private results for LR and GRU-D models on these two tasks as well as implementations.

Suriyakumar et al. (Suriyakumar et al., 2021) replicate Wang et al.’s results on these two tasks for non-private baselines, then provide DPSGD (with RDP accountant) results as well. To the best of our knowledge, Suriyakumar et al. (Suriyakumar et al., 2021) present the state of the art in differentially private ML on these MIMIC-III benchmarks. Unfortunately, their code is not provided.

Using the currently available data (MIMIC-III v1.4, as `all_hourly_data.h5`), and following preprocessing code and descriptions of Wang et al. we replicate these benchmarks as closely as possible. PRV accounting (Gopi et al., 2021) provides a better privacy bound than RDP, and we present comparative results across the two accounting methods. There are discrepancies between our dataset and Suriyakumar et al.’s description of the data, possibly because MIMIC-III was updated. The current MIMIC-III ICU Mortality and Length of Stay benchmarks have 89.1% missingness rate and 104 features per hour  $\times$  24 hours giving 2,496 columns. Suriyakumar et al. claim to have 78% missingness and only 78 features per hour, but they report the number of columns is reported as “24,69”, seemingly a typo (if the correct is 2,496, would entail 104 feature per hour). The number of rows matches exactly. The LR models entails privately learning these 2,497 parameters. We use RMSProp optimizer with a scheduler that reduces the learning rate for all LR models.

For GRU-D, we follow Suriyakumar et al. (Suriyakumar et al., 2021) and when needed the original GRU-D work of Che et al. (Che et al., 2018). Suriyakumar et al. (Suriyakumar et al., 2021) used batch normalization (BN) even when training privately with DPSGD, but this has since been revealed as a source of privacy leakage (Yousefpour et al., 2021).

Hence, we do not use BN with our DPSDG implementations, but we do train a non-private model both with and without BN applied to the top regressor layer. We apply a dropout layer to the top regressor layer, treating the dropout probability as a hyperparameter. Unlike (Suriyakumar et al., 2021), we treat the hidden size as a hyperparameter for all experiments. The main motivation for this choice was that memory constraints on the GPU hardware used to perform ExpM+NF required that we used a hidden size no larger than 10. For the non-private and DPSGD implementations, we allow the hidden size to vary between 10 and 100 for our randomized grid search, so this constraint was only limiting for our new method. For training non-privately and with DPSGD, we use the Adam optimization method and for the NF model we use RMSProp with a scheduler. This is our the best possible replication of Wang et al. and Suriyakumar et al.’s experiments save the choice to omit batch normalization.

Notably, Che et al (Che et al., 2018) also provide non-private GRU-D results on MIMIC-III data for an ICU Mortality prediction task. Since Che et al. do not follow the preprocessing of Wang et al. and specifically claim to use 48 hours of data (while we, Wang, Suriyakumar use 24 hours), we do not consider their results comparable.

We provide benchmark timing results for all three training methods on MIMIC experiments in section 4.2.

## D. Further Results

### D.1. NF Distributions & Discussion

Recall our method is to train an NF model to approximate the ExpM density, which is a density over  $\theta$ , the parameters of our desired classifier. Our results use privacy values for ExpM+NF assuming the NF output is the ExpM distribution. While we cannot visualize the NF’s output distribution (because it is high dimensional), we can investigate the distribution of AUCs attained by ExpM+NF models for each  $\varepsilon$  parameters. We present box plots in which indicate the distribution’s median (middle line), first (Q1) and third (Q3) quartiles (box), and extend 1.5 times the inner quartile range (Q1 - 1.5 IQR, Q3+ 1.5 IQR, whiskers). To see anomalous models arising from fortunate/unfortunate starting positions (different random seeds), we overlay each of the ten model’s means. We also include visualizations of the distribution of the AUC values produced by individual NFs. See Fig. 2. Results are similar across LR and GRU-D, and across both MIMIC-III prediction tasks. Randomness due to the model initialization is exhibited in the variance of each  $\varepsilon$ ’s bar chart. Noise in the hyperparameter search process may influences the distribution trend across  $\varepsilon$  (as a different hyperparameter search is performed for each  $\varepsilon$ ). For this method specifically, outlier NFs can produce bad results based on their randomized initializations. The increase in accuracy and privacy by ExpM+NF also affords a straightforward workaround, e.g., releasing ten models, each sampled from trained NFs with different starting seeds that are then used in a voting scheme.

We found that  $\sigma$ , the hyperparameter governing the variance of the NF’s base distribution, has a large influence on results. Optimal  $\sigma$  found in hyperparameter searches tend to be larger for smaller  $\varepsilon$ , matching the intuition that the NF is more accurate if the base and output distributions’ variance vary together.

The effect of using Sylvester flows (over planar flows) is increased expressiveness, but it comes at the cost of *many* more parameters in the NF model. For example, on the MIMIC-III ICU tasks we have dimension about  $d = 2,500$ . With planar flows, the number of NF parameters needed to train an LR model is  $(2d + 1) \times$  number of flows, which is about 50,000 for 10 flows. With Sylvester flows the number of parameters is roughly  $(d \times k + m^2 + m + d) \times$  the number of flows, where  $k \leq d - 1$  is how many Householder reflections to use and  $m \leq d$  (for planar flows,  $m = 1$ ). If we use  $m = k = 5$  and 10 flows we have about 150,000 NF parameters. Moving to the GRU-D models, we increase  $d$  to the  $\mathcal{O}(50K)$ , so the number of parameters explodes. Future research to understand the gain to accuracy-privacy vs the computational expense incurred by using more expressive NFs for ExpM+NF is needed.

### D.2. Non-Private & DPSGD Advancements

Tables 3 & 4 present non-private LR & GRU-D results, respectively. We find show no significant difference in non-private or DPSGD trained models when using BCE vs.  $\ell^2$  loss. (DPSGD BCE vs.  $\ell^2$  results in Table 1). Note that Wang et al.’s LR used SciKit Learn (Pedregosa et al., 2011) while we use PyTorch.

Table 4 compares results of the GRU-D non-private baseline for previous works and ours, specifically including BCE vs  $\ell^2$  loss and with batch normalization vs. without. We see nearly identical results in our results for each prediction task across the the two loss functions and with/without batch normalization, except for one instance,  $\ell^2$  loss with batch normalization is worse. GRU-D non-private baseline results of our method compared to previous works reside in Table 4. Our results

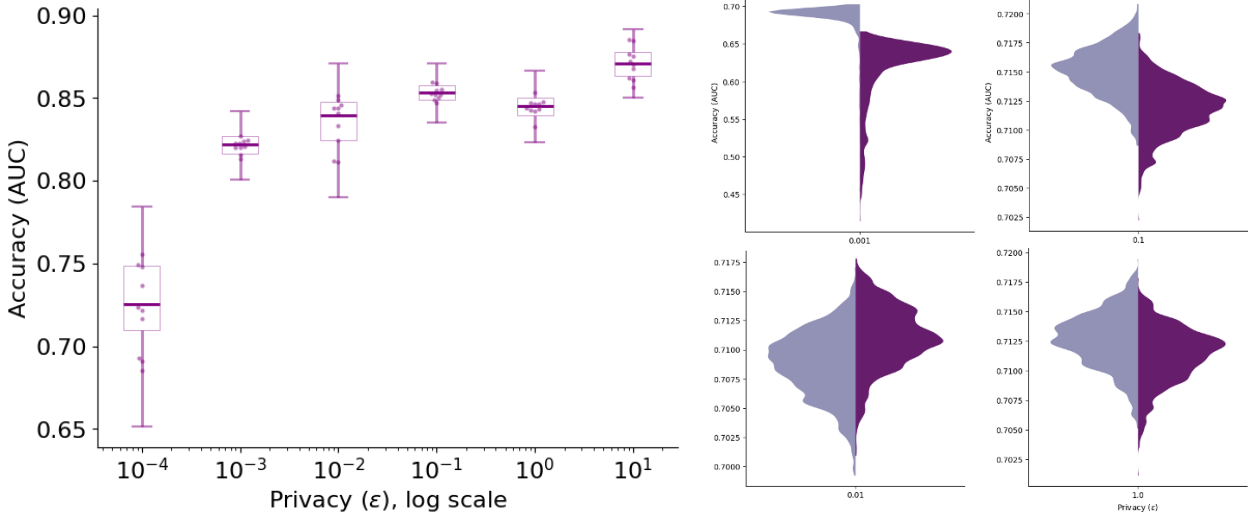


Figure 2: For each  $\varepsilon$  value, ten NF models are trained with identical hyperparameters (but different starting seeds) and used to produce 1,000 samples each from the ExpM distribution. **Right** presents box plots of the 10,000 resulting classifiers’ AUC values. For each NF model’s 1,000 samples we compute the mean AUC, which are overlayed as dots. **Left** presents the AUC distribution from two NFs for four  $\varepsilon$  values.

Table 3: AUC scores for non-private LR model results for this and prior works on MIMIC-III tasks. **Bold** results are best per task. Underlined are the best result in this work.

	(Wang et al., 2020)	(Suriyakumar et al., 2021)	Our $\ell^2$ loss	Our BCE loss
LR, ICU Mortality	<b>.887</b>	.82	<u>.839</u>	.83
LR, Length of Stay	<b>.716</b>	.69	<u>.675</u>	<u>.681</u>

are very close but slightly below Wang et al. (Wang et al., 2020), yet better than Suriyakumar et al. (Suriyakumar et al., 2021). The gains in GRU-D’s performance of ours and Wang et al.’s results may be due to differences in data or other implementation details. Specifically, our hyperparameter search found that a hidden size of about 35-40 performed best, which is much smaller than the 67 hidden size of previous works (Suriyakumar et al., 2021; Che et al., 2018).

Our results show GRU-D, a much more expressive model than LR, does indeed surpass LR in AUC for non-private and each private training method in all experiments, respectively. This trend is seen in Che et al. (Che et al., 2018) and Wang et al. (Wang et al., 2020), but results are the inverse (LR is more accurate) in results of Suriyakumar et al. (Suriyakumar et al., 2021).

We found substantial limitations to the DPSGD RPD accountant compared to the SOTA accounting method, PRV. By using the PRV Accounting method, we achieve state-of-the-art results for DPSGD with both LR and GRU-D models on both ICU Mortality and Length of Stay tasks over the previous works’ health care prediction results (Wang et al., 2020; Suriyakumar et al., 2021). Suriyakumar et al. (Suriyakumar et al., 2021) report LR model AUC for “low privacy” ( $\varepsilon = 3.5e5$ ,  $\delta = 1e-5$ ) and “high privacy” ( $\varepsilon = 3.5$ ,  $\delta = 1e-5$ ) on both ICU Mortality and Length of Stay tasks. Privacy of  $\varepsilon > 10$  is widely considered ineffective (Ponomareva et al., 2023); hence, the “low privacy”  $\varepsilon = 3.5e5$  is practically unreasonable but perhaps useful for investigating sensitivity of this parameter.

Our replication of the same experiment produced LR models trained with DPSGD that greatly improve on this prior state-of-the-art. On ICU Mortality, Suriyakumar et al. (Suriyakumar et al., 2021) report 60% AUC for  $(3.5, 1e-5)$ -DP, whereas we are able to achieve 76% AUC for the same  $(3.5, 1e-5)$ -DP. Our DPSGD implementations are able to achieve 72 – 76% AUC on this task for  $0.5 \leq \varepsilon \leq 10$  and maintain AUC above 60% until  $\varepsilon < 1e-1$ . For the Length of Stay task, Suriyakumar et al. (Suriyakumar et al., 2021) report 60% AUC for  $(3.5, 1e-5)$ -DP, yet our models have 67% AUC for the same  $\varepsilon$ , which is only slightly below the non-private baseline. Again, we do not see an AUC below 60% until  $\varepsilon < 1e-1$ .

Table 4: AUC scores for non-private GRU-D model from this and prior works on MIMIC-III tasks. **Bold** results are best per task. Underlined results are best in this work per task. BN denotes batch normalization.

	(Wang et al., 2020)	(Suriyakumar et al., 2021)	Our $\ell^2$ loss		Our BCE loss	
			BN	No BN	BN	No BN
GRU-D, ICU Mortality	<b>0.891</b>	0.79	0.855	0.875	0.877	<u>0.878</u>
GRU-D, Length of Stay	<b>0.733</b>	0.67	0.721	0.724	0.722	<u>0.722</u>

Much of this improvement can be attributed to using the PRV Accounting method, which allowed us to use much less noise to achieve the same level of privacy.

For the Length of Stay task, Suriyakumar et al. (Suriyakumar et al., 2021) report an AUC of 61% for GRU-D with  $(3.5, 1e-5)$ -DP. We reach 70% AUC with DPSGD for the same level of privacy. This is better than the AUC reported by Suriyakumar et al. (Suriyakumar et al., 2021) for both the non-private LR and GRU-D models and we are able to maintain an AUC greater than 65% for  $\epsilon > 1e-2$  with DPSGD. As we discussed in the prior section, much of the gains in AUC for GRU-D with DPSGD are likely due using the PRV Accounting method. Some of the gains could also be attributed to the same causes that provided the large gains we made for the non-private GRU-D model. Suriyakumar et al. (Suriyakumar et al., 2021) show a sharp decrease in AUC when training GRU-D with DPSGD on ICU Mortality task, even in the “low privacy” case with  $\epsilon = 3e5$ . They report 59% AUC for this high  $\epsilon$  and 53% AUC for the “strong privacy” case,  $(3.5, 1e-5)$ -DP, which is not much better than random guessing. Our DPSGD PRV implementation of GRU-D achieves median 82.7% AUC for  $(3.5, 1e-5)$ -DP using GRU-D on the Mortality prediction task. This is comparable to the best non-private LR model that we achieved, and is better than the performance (Suriyakumar et al., 2021) reported for non-private GRU-D. Our DPSGD results achieve AUC greater than 60% for each  $\epsilon > 1e-2$  in this prediction task.

### D.3. Training Time Details

The details of this subsection correspond with performance results in Sec. 4.2. As all our models are implemented in PyTorch, we use PyTorch’s benchmark suite over ten runs on a single NVIDIA A100 80GB GPU and 128 CPUs with 2TB of shared RAM. For DPSGD and ExpM+NF, we additionally take the mean across the various privacy levels, noting that some  $\epsilon$  may have hyperparameters that led it to take more or less time than this reported mean. For the non-private GRU-D implementation, we report mean training time with batch normalization which took less time. In the case of the non-private BCE loss, the number of epochs and batch size were larger, likely attributing to the increased training time.

Table 5: Length of Stay Benchmark Timing Results

Task	Loss	Logistic Regression			GRU-D		
		Training Time	Computing $\epsilon$	Total	Training Time	Computing $\epsilon$	Total
Non- Private	$\ell^2$	1.57 ms	—	1.57 ms	.81 ms	—	.81 ms
	BCE	1.51 ms	—	1.51 ms	1.46 ms	—	1.46 ms
DPSGD	$\ell^2$	1.41 ms	1.36 ms	2.77 ms	1.8 ms	1.5 ms	3.3 ms
	BCE	1.36 ms	1.3 ms	2.63 ms	1.67 ms	1.76 ms	3.45 ms
ExpM+NF	RKL+ $\ell^2$	1.74 ms	—	1.74 ms	1.81 ms	—	1.81 ms